Immunomodulatory effects exerted by extracellular vesicles from Staphylococcus epidermidis and Staphylococcus aureus isolated from bone-anchored prostheses

Zaborowska, Magdalena; Vazirisani, Forugh; Shah, Furqan A.; Firdaus, Rininta; Omar, Omar; Ekström, Karin; Trobos, Margarita; Thomsen, Peter

DOI:
10.1016/j.biomaterials.2021.121158

Document Version
Publisher's PDF, also known as Version of record

Citation for published version (Harvard):
Zaborowska, M, Vazirisani, F, Shah, FA, Firdaus, R, Omar, O, Ekström, K, Trobos, M & Thomsen, P 2021, 'Immunomodulatory effects exerted by extracellular vesicles from *Staphylococcus epidermidis* and *Staphylococcus aureus* isolated from bone-anchored prostheses', *Biomaterials*, vol. 278, 121158. https://doi.org/10.1016/j.biomaterials.2021.121158

Biomaterials 278 (2021) 121158

Contents lists available at ScienceDirect

Biomaterials

journal homepage: www.elsevier.com/locate/biomaterials

Immunomodulatory effects exerted by extracellular vesicles from *Staphylococcus epidermidis* and *Staphylococcus aureus* isolated from bone-anchored prostheses

Magdalena Zaborowska [a,b], Forugh Vazirisani [a,b], Furqan A. Shah [a], Rininta Firdaus [a,b], Omar Omar [a], Karin Ekström [a], Margarita Trobos [a,b], Peter Thomsen [a,*]

[a] Department of Biomaterials, Institute of Clinical Sciences, Sahlgrenska Academy, University of Gothenburg, Gothenburg, Sweden
[b] Center for Antibiotic Resistance Research (CARe), University of Gothenburg, Gothenburg, Sweden

ARTICLE INFO

Keywords:
Chemokines
Cytokines
Cytotoxicity
Biomaterial-associated infection
Extracellular vesicles
Monocyte
Macrophage
Inflammation
Staphylococci
THP-1

ABSTRACT

Staphylococcus aureus and *Staphylococcus epidermidis* are the bacteria that most frequently cause osteomyelitis. This study aimed to determine whether staphylococci isolated from osteomyelitis associated with septic loosening of orthopedic prostheses release extracellular vesicles (EVs) and, if so, to determine tentative immunomodulatory effects on the human monocytic cell line THP-1. EVs were isolated from bacterial cultures using filtration and ultracentrifugation and characterized by scanning electron microscopy, nanoparticle tracking analysis and Western Blot. The cytotoxic effect of EVs was analyzed by NucleoCounter and lactate dehydrogenase (LDH) analyses. Confocal laser scanning microscopy was employed to visualize the uptake of EVs by THP-1 cells. Activation of the transcription factor nuclear factor-κB (NF-κB) was determined in THP1-Blue™ NF-κB cells, and the gene expression and secretion of cytokines were determined by quantitative polymerase chain reaction and enzyme-linked immunosorbent assay, respectively. All investigated strains, irrespective of their biofilm formation ability, were able to secrete EVs *in vitro*. The *S. aureus* strains produced significantly more EVs than the *S. epidermidis* strains. Both *S. aureus*-derived EVs and *S. epidermidis*-derived EVs were internalized by THP-1 cells, upregulated Toll-like receptor 3 (TLR3) gene expression, activated NF-κB, and promoted the gene expression and secretion of interleukin (IL)-8, monocyte chemoattractant protein (MCP)-1, matrix metallopeptidase (MMP)-9 and IL-10. Whereas EVs from both staphylococcal species upregulated the proapoptotic DNA damage-inducible transcript 4 (DDIT4) gene and downregulated the antiapoptotic B-cell lymphoma 2 (Bcl-2) gene, cytolysis was preferentially induced in *S. aureus* EV-stimulated cells, possibly related to the expression of cytolytic proteins predominantly in *S. aureus* EVs. In conclusion, staphylococcal EVs possess potent cytolytic and immunomodulatory properties.

1. Introduction

The implantation of a material in the body initiates a series of intertwined biological events, including initial inflammation, which involves the recruitment of monocytes and macrophages, followed by repair and regeneration of the injured tissue in association with the implant [1]. The interactions between the surface of the material and factors of the coagulation and complement systems and cells influence the outcome of implantation. Multiple cell types are involved, although their appearance, activities and major roles may typically peak at a specific time point after implantation [2]. Neither the mechanisms underlying successful and lasting implantation nor the mechanisms of aseptic or septic loosening of bone-anchored prostheses are fully understood.

Currently, major efforts are focused on the prevention, diagnosis and treatment of biomaterial-associated infection [3]. In addition to antimicrobial modifications of prosthetic surfaces, local implant-related immune "exhaustion", staphylococcal invasion of host cells and bone, production of toxins and formation of biofilms are processes that include targets for intervention [4]. *Staphylococcus aureus* and the opportunistic pathogen *Staphylococcus epidermidis* are common causes of implant-associated infections (*e.g.,* periprosthetic orthopedic infections)

* Corresponding author.
E-mail address: peter.thomsen@biomaterials.gu.se (P. Thomsen).

https://doi.org/10.1016/j.biomaterials.2021.121158
Received 10 May 2021; Received in revised form 11 September 2021; Accepted 27 September 2021
Available online 28 September 2021

[5–7]. The consequences of these infections include surgery and/or long-term treatment with antimicrobial agents, which inflict a major burden and costs for the individual and society [6,7]. Periprosthetic orthopedic infections are often believed to be biofilm-mediated infections that are difficult to treat due to persister cells within the biofilm [8,9].

The host response defending against bacterial pathogens includes leukocyte migration, phagocytosis and killing of pathogens by inflammatory cells. Immune cells secrete proinflammatory cytokines and chemokines, including tumor necrosis factor (TNF)-α, interleukin (IL)-1β, IL-8, IL-6, and monocyte chemoattractant protein (MCP)-1, to recruit other inflammatory cells to combat bacterial pathogens [10]. In addition to proinflammatory cytokines, anti-inflammatory cytokines, such as IL-10, are secreted. The inflammatory response triggered by a persistent biofilm eventually causes host tissue damage since it becomes chronic [9].

The ability to form a biofilm is one of several virulence mechanisms of pathogenic bacteria to evade immune defense, and another is secretion of virulence factors, such as enzymes and toxins. How these virulence factors are delivered is not fully understood [11]. However, it is well known that a wide variety of species of gram-negative bacteria secrete spherical outer membrane vesicles (OMVs) with an average diameter of 20–200 nm containing virulence factors, genetic material, and membrane-associated proteins that are delivered to host cells to elicit a cytotoxic effect [12–14]. In recent years, gram-positive bacteria have also been shown to produce extracellular vesicles (EVs), and it has been demonstrated that EVs derived from *S. aureus* contain various lipids and proteins, such as toxins and adhesion molecules, and other tissue-destructive enzymes [11,15–17]. This suggests that EVs secreted from *S. aureus* may be associated with the development or progression of diseases. To our knowledge, no studies regarding the secretion of EVs by clinical staphylococcal isolates derived from implant-related osteomyelitis have been performed. Furthermore, there is no available information on whether *S. epidermidis* secretes EVs or whether such EVs possess similar or dissimilar biological properties compared to *S. aureus*-derived EVs. The aims of this study were to determine (i) whether staphylococci isolated from human implant-related osteomyelitis release EVs and (ii) whether these EVs elicit THP-1 cell cytolysis and proinflammatory cytokine secretion.

2. Materials and methods

2.1. Bacterial strains and eukaryotic cells

Staphylococci strains including three *S. epidermidis* (CCUG64518, CCUG64521, and CCUG64523) and four *S. aureus* (CCUG64514, CCUG64516, CCUG64520, and CCUG64522) strains were isolated from bone biopsies, bone marrow aspirates and inner implant components in a cohort of seven patients with bone-anchored transfemoral amputation prostheses diagnosed with osteomyelitis between March 2008 and April 2012. The isolates were freeze dried and stored at the Clinical Bacteriological Laboratory at Sahlgrenska University Hospital (Gothenburg, Sweden) and the Culture Collection University of Gothenburg (CCUG) (Gothenburg, Sweden). The reference bacterial strains *S. epidermidis* ATCC12228, *S. epidermidis* ATCC35984 and *S. aureus* ATCC25923 and the eukaryotic cell line THP-1 (ATCC TIB202) were purchased from ATCC (ATCC, Manassas, VA, USA). The use of clinical strains in this study was approved by the Regional Ethical Review Board in Gothenburg (Dnr. 434–09). A summary of patient demographics and strain characteristics is found in Table 1.

2.2. Isolation of EVs from planktonic cultures of staphylococci

One colony from overnight cultures grown on 5% horse blood Columbia agar plates (Media Department, Clinical Microbiology Laboratory, Sahlgrenska University Hospital (Gothenburg, Sweden) was subcultured in 100 mL tryptic soy broth (TSB) (Eur. Pharm. Scharlau, Spain) and incubated at 37 °C for 22 h with gentle shaking (125 rpm). Bacterial cells were removed from the cultures by centrifugation at 3000*g* for 20 min at 4 °C. The culture supernatants were sequentially filtered through 0.45- and 0.22-μm pore-size vacuum filters (Sarstedt AG & Co., Nümbrecht, Germany) to remove the remaining bacterial cells. Sterility was checked by spreading cultures of 100 μL supernatant onto blood agar plates. The bacteria-free liquid was concentrated by ultrafiltration with a 100-kDa hollow fiber membrane using the ÄktaFlux Benchtop System (GE Healthcare Bio-Sciences AB, Uppsala, Sweden). The concentrated liquid was kept frozen at −80 °C until it was centrifuged at 16,500 *g* for 20 min, and the supernatant was filtered with 0.22-μm pore-size vacuum filters (Sarstedt, Nümbrecht, Germany). The supernatant was ultracentrifuged at 150,000 *g* for 3 h at 4 °C in a T-647.5 rotor (Sorvall wx Ultra series, Thermo Scientific, USA) to pellet EVs. The resulting vesicle pellet was washed in phosphate-buffered saline (PBS), centrifuged at 150,000 *g* for 3 h at 4 °C and resuspended in PBS. Three separate batches of EVs per bacterial strain were isolated. EVs were stored at −80 °C until further use.

2.3. Characterization of EVs

2.3.1. Nanoparticle tracking analysis

Isolated EVs were analyzed using a NanoSight LM10/LM14 instrument (NanoSight Ltd., Amesbury, UK). EVs were diluted in PBS, injected into the LM14 module and captured 3 × 60 s. EV samples were evaluated

Table 1
A summary of patient demographics and strain characteristics (based on previously published data in Zaborowska et al., 2016 [58]).

Causative strains	Patient demographics				Strain characteristics			
	Time of infection after implantation (years)	Reinfection	Relapse	Extraction	Biomass score	Slime score	Biofilm production score	Biofilm production classification
S. epidermidis clinical strains								
CCUG64518	12	No	No	Yes	3	1	4	Moderate
CCUG64521	3	Yes	No	No	3	2	5	Strong
CCUG64523	0	No	No	No	2	0	2	Nonproducer
S. aureus clinical strains								
CCUG64514	12	No	Yes	No	2	2	4	Moderate
CCUG64516	5	No	No	Yes	2	2	4	Moderate
CCUG64520	3	Yes	No	No	2	0	2	Nonproducer
CCUG64522	3.5	Yes	Yes	No	1	2	3	Weak
Reference strains								
S. epidermidis ATCC35984	–	–	–	–	3	2	5	Strong
S. epidermidis ATCC12228	–	–	–	–	2	0	2	Nonproducer
S. aureus ATCC25923	–	–	–	–	1	2	3	Weak

in triplicate. Videos were then subjected to nanoparticle tracking analysis (NTA) using NanoSight particle tracking software 3.1 to determine nanoparticle concentrations and size distribution profiles (mean and standard error of the mean from 3 × 3 captures). This was performed for each EV batch for each of the different strains. The mean and standard error of the mean were calculated for each strain.

2.3.2. Protein quantification

The EV protein concentration was quantified using the Pierce® BCA Protein Assay Kit (Thermo Scientific, Rockford, USA) following the manufacturer's instructions.

2.3.3. SDS PAGE and western blot (WB)

EVs from *S. epidermidis* (CCUG 64518, CCUG 64521, CCUG 64523, ATCC 35984, ATCC 12228) and *S. aureu* (CCUG 64514, CCUG64520, CCUG 64522, CCUG 645, ATCC 25923) were dissolved in Laemmli or Tricine sample buffer (Bio-Rad Laboratories, Hercules, CA, USA) and heated at 95 °C for 5 min. A total of 10 μg of EV proteins were loaded per well onto 10% TGX and Tris-Tricine Mini-protean precast gels (Bio-Rad) alongside with Precision Plus Protein™ WesternC™ Blotting Standards (Bio-Rad). The running time of SDS PAGE was 1 h at 130 V. Further, the gels were transferred to nitrocellulose membranes (BioRad) on a semi-dry transfer system. The membranes were blocked for 1.5 h with 2% non-fat milk powder (Bio-Rad) in Tris-Buffered Saline-Tween (TBS-T) at RT. The membranes were incubated with the following primary antibodies: rabbit polyclonal anti-Staphylococcal α-toxin (S7531, Sigma-Aldrich, Darmstadt, Germany, 1:500), rabbit polyclonal anti-δ-toxin (USBiological Life Sciences, Swampscott, USA, 1:500), rabbit polyclonal anti-Protein A (P3775, Sigma-Aldrich, 1:1000), and rabbit polyclonal anti-Staphopain A (ab92983, Abcam, Cambridge, UK, 1:500) antibodies at 4 °C overnight. The membranes were washed 3 × 5 min in TBS-T prior to incubation with HRP-conjugated goat anti-rabbit secondary antibody (sc-2004, Santa Cruz Biotechnology, Santa Cruz, USA, 1:10,000) for 1 h at RT. All antibodies were diluted in 2% non-fat milk powder in TBS-T. Finally, the membranes were washed 3 × 15 min in TBS-T followed by the development with Clarity™Western ECL Substrate detection kit (Bio-Rad) for 5 min. Digital detection was made using the ChemiDoc XRS + system with Image Lab Software (Bio-Rad).

2.3.4. Scanning electron microscopy

A volume of 10 μL EV, corresponding to a protein concentration of 0.5–1 μg × μL^{-1} in filtered PBS, was loaded onto 200 mesh Cu 01700-F formvar carbon-coated grids (Ted Pella Inc, Redding, CA, USA). After 1 h, the samples were washed, fixed in 2% paraformaldehyde for 10 min, washed in PBS, postfixed in 2.5% glutaraldehyde, washed in distilled H_2O and negatively stained with 2% uranyl acetate for 15 min. The samples were dried, Au sputter coated (≈10 nm) and examined using scanning electron microscopy (SEM) (Ultra 55 FEG SEM, Leo Electron Microscopy Ltd, UK) in the secondary electron mode, operated at a 5-kV accelerating voltage and 10-mm working distance.

2.4. Stimulation of human monocytes

For a stimulation assay, the human monocytic cell line THP-1 (ATCC, Manassas, USA) was propagated in Roswell Park Memorial Institute (RPMI) 1640 medium supplemented with 10% fetal bovine serum (FBS) (Sigma Aldrich, Munich, Germany), 1% antibiotic-antimycotic solution (Gibco, Life Technologies, Carlsbad, CA, USA) and 0.05 mM 2-mercaptoethanol in a 37 °C humidified incubator with 5% CO_2. THP-1 monocytes were seeded at a density of 500,000 cells per mL in Nunc 24-well plates (Thermo Fisher Scientific, Roskilde, Denmark) in 1 mL RPMI 1640 medium supplemented with 10% FBS without antibiotics and stimulated with increasing protein concentrations (0, 5 and 25 μg × mL^{-1}) of *S. epidermidis* or *S. aureus* EVs derived from the clinical strains. Monocytes stimulated with the gram-positive *S. aureus* cell wall component lipoteichoic acid (LTA) (Sigma-Aldrich, Munich, Germany) (5 μg × mL^{-1}) served as a positive control. Monocytes stimulated with medium alone served as a negative control. The proportions of viable and dead cells were determined using propidium iodide (PI) staining evaluated with a NucleoCounter NC-100 system (ChemoMetec A/S, Allerød, Denmark) after 24 h of stimulation. Each experiment was performed with triplicate samples and repeated three times. One batch of EVs per separate trial was used. The supernatant was harvested from each well, centrifuged to remove cells at 400 g for 5 min, aliquoted for analysis of lactate dehydrogenase (LDH) and stored at −80 °C for subsequent enzyme-linked immunosorbent assays (ELISAs). Cell pellets were stored in RLT buffer at −80 °C for gene expression analysis.

2.5. LDH analysis

The levels of LDH released by cells into the cell supernatant were analyzed to assess the degree of cytotoxicity. The analysis used spectrophotometric evaluation of the LDH-mediated conversion of pyruvic acid into lactic acid (C-Laboratory, Sahlgrenska University Hospital, Gothenburg, Sweden).

2.6. Quantitative polymerase chain reaction (qPCR)

Total RNA was isolated from samples with an RNeasy Micro kit (Qiagen, Hilden, Germany) according to the manufacturer's instructions. The isolated RNA was reverse transcribed into cDNA using the High Capacity cDNA Reverse Transcription Kit (Life Technologies). Each qPCR reaction was performed using cDNA equivalent to 2.5 ng RNA, TaqMan Universal PCR Master Mix and 1 × mixes of primers and TaqMan MGB probes. The gene panel included the following genes: IL-8, MCP-1, IL-10, IL-6, Toll-like receptor-2 (TLR2), Toll-like receptor 3 (TLR3), Toll-like receptor 4 (TLR4), DNA damage-inducible transcript 4 (DDIT4) and B-cell lymphoma 2 (Bcl-2). All samples were analyzed in duplicate, and reactions were performed using a 7900HT real-time PCR system (Life Technologies). Quantification of relative target gene expression was performed according to a standard curve and the ΔΔ-Cq method using 18 S rRNA as a reference gene.

2.7. Cytokine secretion (ELISA)

Supernatants stored at −80 °C were used to determine the concentrations of IL-8, IL-10, MCP-1 and matrix metallopeptidase 9 (MMP-9) using ELISA according to the manufacturer's instructions (Quantikine ELISA, R&D Systems™, Minneapolis, MN, USA). All samples were measured in triplicate in three separate trials.

2.8. Cellular NF-κB activation assay

THP1-Blue™ NF-κB cells (InvivoGen, Toulouse, France), originally derived from monocytic THP-1 cells and carrying a stable integrated nuclear factor (NF)-κB-inducible secreted embryonic alkaline phosphatase (SEAP) reporter construct, were used to analyze NF-κB induction. Cells were propagated in RPMI 1640 medium supplemented with 10% FBS and 100 μg × mL^{-1} Normacin™. Approximately 50,000 cells × mL^{-1} suspended in 1 mL RPMI 1640 medium supplemented with 10% FBS without antibiotics were pipetted into 96-well plates. The cells were stimulated with *S. epidermidis* EVs from the strain CCUG 64521 or *S. aureus* EVs from the strain CCUG 64516 at 5 and 25 μg × mL^{-1}. Heat-killed *Listeria monocytogenes* (provided in the kit) and endotoxin-free water served as the positive and negative controls, respectively. The cells were incubated in a 37 °C humidified incubator with 5% CO_2 for 6, 12, and 24 h. QUANTI-Blue™ Solution was added to a new 96-well plate in a volume of 180 μL, the cell supernatants (20 μL) were added to the plate and incubated for 1–2 h, and the optical density was measured at 655 nm.

2.9. Internalization of EVs by THP-1 cells

EVs derived from the clinical *S. aureus* CCUG64520 and *S. epidermidis* CCUG64523 strains were diluted in 500 μL RPMI 1640 medium, and 2.5 μL DiO dye (Molecular Probes, Eugene, OR, USA) was added and incubated for 30 min at 37 °C. After incubation, the samples were transferred to 1.5-mL 100-kDa filters (Millipore, Massachusetts, USA) and washed three times with PBS at 14,000 *g* according to the manufacturer's instructions. The filters were inverted and centrifuged at 1000 *g* to collect the labeled EVs. The collected EVs were kept at 8 °C until use the next day. DiO added to PBS, stained and washed in parallel to the prepared EVs served as a control.

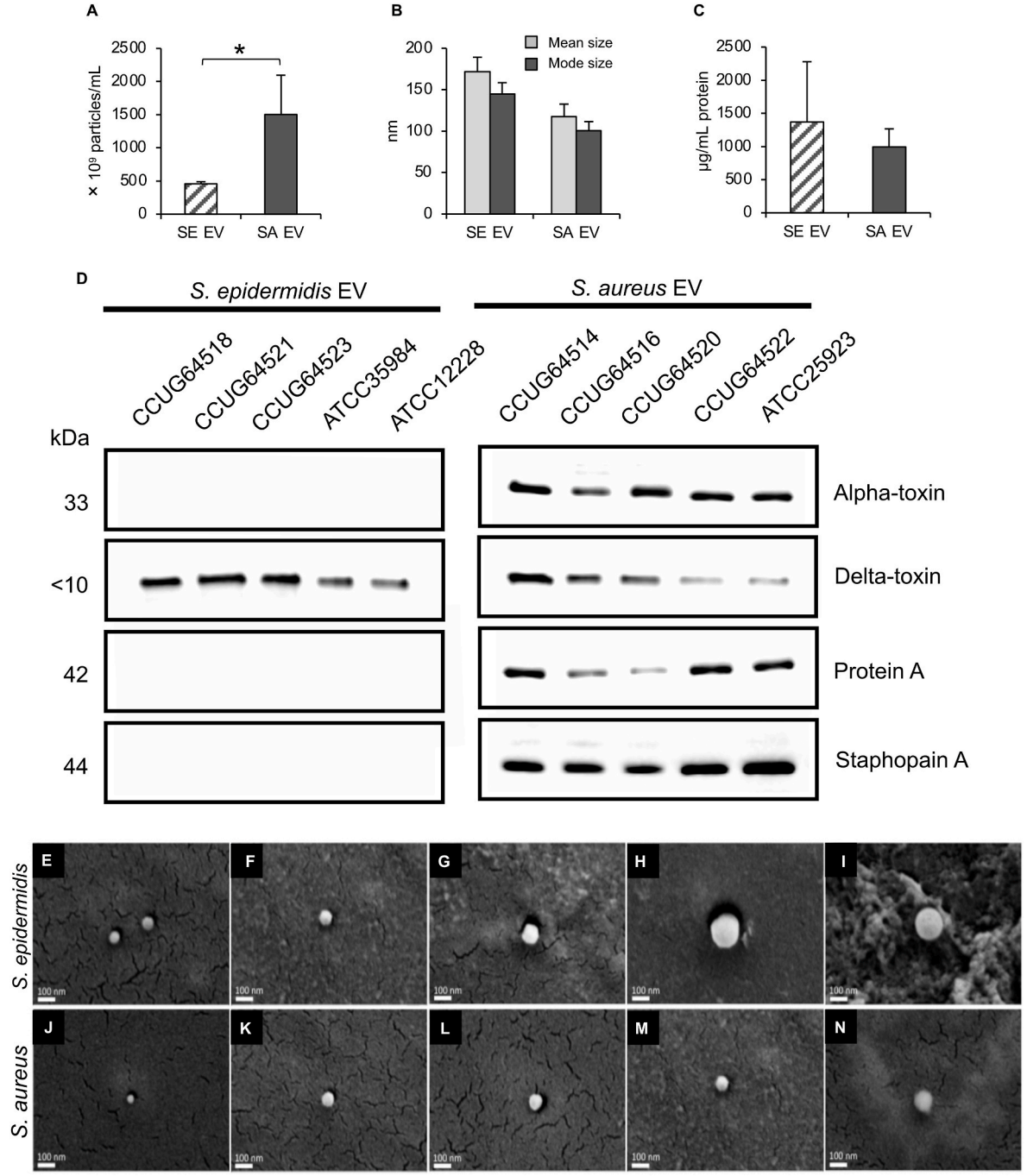

Fig. 1. Characterization of *Staphylococcus epidermidis* and *Staphylococcus aureus* EVs by nanoparticle tracking analysis. A) Averaged particle concentrations of EVs derived from *S. epidermidis and S. aureus* clinical strains. B) Mean and mode sizes of EVs derived from *S. epidermidis and S. aureus* clinical strains. C) Averaged protein concentrations of EVs derived from *S. epidermidis and S. aureus* clinical strains (Total protein amount of EVs). D) Qualitative characterization of proteins in EVs from the individual clinical and reference strains of *S. epidermidis* and *S. aureus* by Western blot. Ten micrograms of EVs were lysed in Laemmli or Tricine sample buffer and separated on 10% Tris-Glycine or Tris-Tricine SDS-PAGE gel. After transfer to nitrocellulose membrane, blots were probed with anti-Staphylococcal α-toxin (1:500), anti-δ-toxin (1:500), anti-Protein A (1:1000), and anti-Staphopain A (1:500) antibodies. Subsequent detection was carried out with anti-rabbit HRP (1:10,000). E-N) Scanning electron microscopy images of EVs derived from the clinical *S. epidermidis* strains E-G) CCUG64518, CCUG64521, and CCUG64523; H–I) EVs derived from the reference *S. epidermidis* strains ATCC35984 and ATCC12228; EVs isolated from the clinical *S. aureus* strains J-M) CCUG64514, CCUG64516, CCUG64520, and CCUG64522; and N) EVs derived from the reference *S. aureus* strain ATCC25923. The error bars show the standard error of the mean; $n = 3$ biological replicates. Significant difference between EVs of different origins is indicated by asterisk: *$p < 0.05$.

THP-1 cells were stained with DiI (Molecular Probes, Eugene, OR, USA) according to the manufacturer's protocol. In brief, 5 μL DiI was added per milliliter of cell suspension containing 1×10^6 cells $\times$ mL^{-1} and incubated for 15 min at 37 °C. The cells were washed three times with culture medium to remove any unbound stain. The DiI-labeled cells were seeded in a Nunc 24-well plate at a concentration of 5×10^5 cells $\times$ mL^{-1}. EVs stained with DiO at concentrations of 5 and 25 μg $\times$ mL^{-1} were added to the cells and incubated at 37 °C for 4 h. One hundred microliters of cell suspension (approximately 1×10^5 cells) was applied to microscopy slides using cytospin centrifugation (Shandon, Runcorn, UK). The cells were fixed with 2% formaldehyde for 15 min and washed twice in PBS before being mounted with Vectashield HardSet Mounting Medium with 4′,6-diamidino-2-phenylindole (DAPI; Vector Laboratories, Burlingame, USA). The samples were analyzed with a Nikon C2 confocal laser scanning microscope (CLSM; Nikon, Tokyo, Japan). The experiment was repeated three times with two technical replicates.

2.10. Statistical analysis

Differences in EV number, size (NTA) and protein concentration (NanoDrop) were analyzed by one-way analysis of variance (ANOVA) followed by Fisher's least significant difference (LSD) post hoc test. Differences between EV-stimulated groups and the nonstimulated or LTA-stimulated control groups were analyzed with the Kruskal-Wallis test followed by the Mann-Whitney *U* test. Differences between different concentrations of EVs from the same species were analyzed with an independent sample *t*-test. For all tests, differences were considered significant at $p < 0.05$. Mean values ± standard error of the mean are presented. Statistical analyses were performed using SPSS Statistics, v. 21 (IBM Corporation, USA).

3. Results

3.1. NTA

As judged by NTA measurements, the number of EVs obtained from the clinical *S. aureus* strains was significantly higher than that of EVs isolated from the *S. epidermidis* strains ($1.50 \times 10^{12} \pm 1.19 \times 10^{12}$ particles per mL and $4.57 \times 10^{11} \pm \times 5.64\ 10^{10}$ particles per mL, respectively) (Fig. 1A). *S. epidermidis* (mean 172 ± 17 nm; mode 117 ± 13 nm) and *S. aureus* (mean 145 ± 15 nm; mode 100 ± 11 nm) EVs were similar in size (Fig. 1B). Full EV characterization data generated by NTA (particle concentration and size) for each clinical and reference strain are presented in Supplementary Figure S1 and S2A.

3.2. EV protein content

The content of proteins in clinical EV isolates was determined by the Pierce™ BCA Protein Assay and nanospectrophotometry (Fig. 1C). No significant differences in protein content were found between *S. epidermidis* EVs and *S. aureus* EVs. Full EV characterization data with respect to protein content for each clinical and reference strain are presented in Supplementary Figure S2B.

3.3. WB

Proteins in EVs were qualitatively assessed by Western blot analysis. Four antibodies against staphylococcal proteins were used including α-toxin, δ-toxin, Protein A, and Staphopain A (Fig. 1D). Only δ-toxin was detected in the *S. epidermidis* EVs from clinical strains (CCUG 64518, CCUG 64521, CCUG 64523) and reference strains (ATCC 35984 and ATCC 12228). In contrast, α-toxin, δ-toxin, Protein A and Staphopain A were all detected in *S. aureus* EVs from clinical strains (CCUG 64514, CCUG 64516, CCUG 64520, CCUG 64522) and reference strain (ATCC 25923).

3.4. SEM

SEM was used for qualitative analysis of isolated pellets. SEM confirmed the presence of isolated EVs from all three clinical *S. epidermidis* strains, two reference ATCC *S. epidermidis* strains, four clinical *S. aureus* strains and one reference ATCC *S. aureus* strain (Fig. 1E-N). The EVs appeared roughly spherical with some irregularities at the periphery, which were attributable to sample preparation and deformation under the electron beam.

3.5. Cell viability

The viability of THP-1 cells after exposure to EVs was determined using NucleoCounter (Fig. 2A) and LDH (Fig. 2B) analyses. By NucleoCounter analysis, a significantly higher decrease in cell viability was shown for both concentrations of *S. aureus*-derived EVs (5 and 25 μg $\times$ mL^{-1}) than for nonstimulated control treatment (Fig. 2A). The high dose of *S. aureus* EVs caused a significantly greater decrease of viability than LTA. In addition, the viability of THP-1 cells was significantly reduced after stimulation with the highest concentration of *S. aureus* EVs compared with stimulation with the lowest concentration (Fig. 2A). The *S. epidermidis* EV-stimulated group (25 μg $\times$ mL^{-1}) had significantly lower THP-1 cell viability than the nonstimulated control group; however, no significant difference was observed compared with the LTA group. The decrease in the viability of THP-1 cells in the *S. epidermidis* EV (5 μg $\times$ mL^{-1})-stimulated group did not differ significantly from that in the negative and positive control groups. No significant difference in NucleoCounter-determined cell viability was detected between the *S. epidermidis* EV- and *S. aureus* EV-treated groups.

A significantly higher increase in LDH in the supernatant (indicative of cytolysis) was observed in cultures of THP-1 cells stimulated with 5 or 25 μg $\times$ mL^{-1} *S. aureus* EVs compared with those stimulated with the negative or positive control (Fig. 2B). EVs from *S. aureus* induced significantly higher (≈2-fold) LDH release than the equivalent concentrations of *S. epidermidis* EVs. No statistically significant differences in LDH were observed between *S. epidermidis* EVs and the negative control or LTA.

Full data on THP-1 cell viability changes induced by EVs from all individual clinical and reference strains, are shown in Supplementary Figure S3. No significant differences in cell viability or LDH release were observed between the test strains and reference strains.

3.6. Gene expression

The gene expression of IL-8, MCP-1, MMP-9, and IL-10 after stimulation with EVs was significantly higher (50- to 2000-fold) than that observed with unstimulated control or LTA treatment irrespective of the EV origin and concentration (Fig. 3A–D). Furthermore, similar findings were found for IL-6 (Fig. 3E). For both *S. epidermidis*-derived EVs and *S. aureus*-derived EVs, significantly higher expression of IL-8 and IL-6 was demonstrated for the highest concentration (25 μg $\times$ mL^{-1}) used. In contrast, for MCP-1 and IL-10, such a finding was detected only when *S. aureus* EVs were administered. No concentration-dependent difference was observed for MMP-9 gene expression. LTA induced significantly higher expression of MCP-1 and IL-10 than the negative control.

Gene expression data for TLR2, TLR3 and TLR4 are presented in Fig. 3F–H. A significant (20- to 280-fold) increase in the expression of TLR3 was demonstrated for both *S. epidermidis* EVs and *S. aureus* EVs compared with the negative control, irrespective of the EV concentration (Fig. 3G). Similarly, significantly higher expression of TLR3 was found for all EV groups except for the *S. epidermidis* EVs at 5 μg $\times$ mL^{-1} group compared with the LTA group. A similar pattern was found for TLR2, revealing higher expression induced with *S. aureus* EVs (both concentrations) or *S. epidermidis* EVs (25 μg $\times$ mL^{-1}) compared to the controls, although the differences were not statistically significant (Fig. 3F). No significant differences were detected among the groups

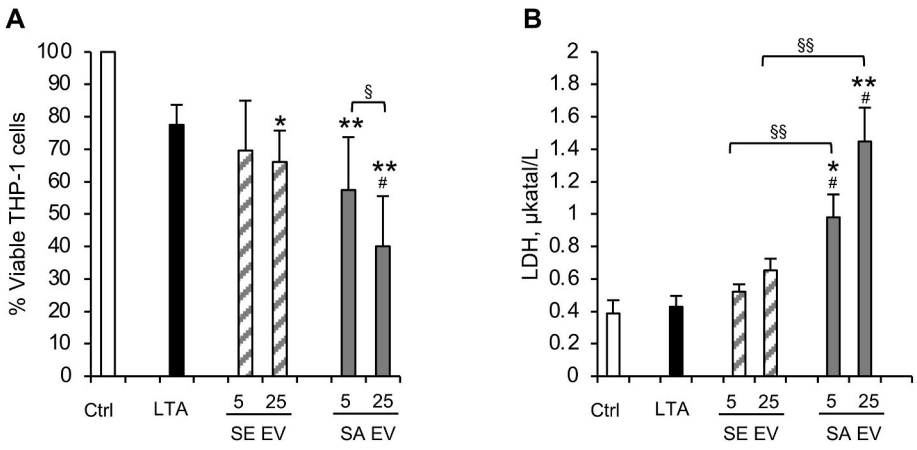

Fig. 2. A) Percentage of viable THP-1 cells and B) concentration of LDH after a 24-h incubation with medium only (control; Ctrl), 5 μg × mL^{-1} lipoteichoic acid (LTA), or 5 μg × mL^{-1} or 25 μg × mL^{-1} EVs derived from clinical *S. epidermidis* (SE) or *S. aureus* (SA) strains. Error bars show the standard error of the mean; $n = 3$ biological replicates. The bars for SE and SA represent the mean of 3 separate trials of each of the three (SE) and four (SA) strains, respectively. Significant differences compared to control are indicated by asterisks: *p < 0.05; **<0.01. Significant differences compared to LTA are indicated by hash sign: #p < 0.05. Significant differences between different EV concentrations or EVs of different origins for an equivalent concentration are indicated by section signs: §<0.05; §§<0.01.

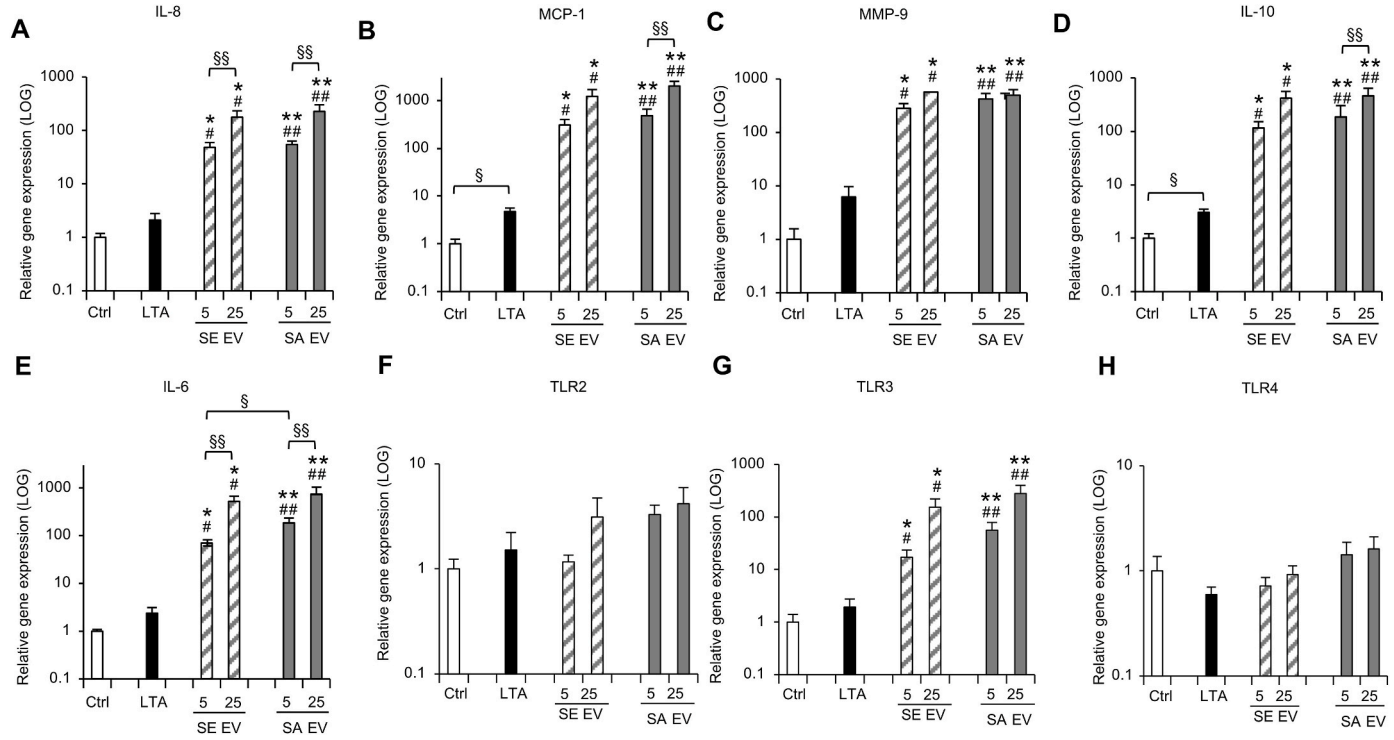

Fig. 3. The gene expression of THP-1 cells after a 24-h incubation with medium only (control; Ctrl), 5 μg × mL^{-1} lipoteichoic acid (LTA), or 5 μg × mL^{-1} or 25 μg × mL^{-1} *S. epidermidis* (SE)- or *S. aureus* (SA)-derived EVs determined by qPCR. A) IL-8, B) MCP-1, C) MMP-9, D) IL-10, E) IL-6, F) TLR2, G) TLR3 and, H) TLR4. Error bars show the standard error of the mean; $n = 3$ biological replicates. The bars for SE and SA represent the mean of 3 separate trials of each of the three (SE) and four (SA) clinical strains, respectively. Significant differences compared to control are indicated by asterisks: *p < 0.05; **<0.01. Significant differences compared to LTA are indicated by hash signs: #p < 0.05; ##p < 0.01. Significant differences between different EV concentrations or EVs of different origins for an equivalent concentration are indicated by section signs: §<0.05; §§<0.01.

with respect to TLR4 gene expression (Fig. 3H). The expression of DDIT4 was significantly higher (10- to 100-fold) in all EV-stimulated groups than in the LTA group (Fig. 4A). A similar trend of elevated DDIT4 expression (5- to 50-fold) was detected for all EV-stimulated groups compared to the negative control group, but the difference was not significant. The LTA group demonstrated 2-fold lower expression of DDIT4 than the negative control group. In contrast to the results for DDIT4, all EV-stimulated groups, irrespective of species and concentration, showed significantly lower (6- to 9-fold) Bcl-2 expression than both the negative control and LTA groups (Fig. 4B).

3.7. Protein secretion

The overall amounts of secreted IL-8, MCP-1, MMP-9 and IL-10 were analyzed in the culture media of the different experimental groups after 24 h of culture. EVs derived from both species promoted the secretion of IL-8 by THP-1 cells (Fig. 5A). The highest concentration induced ≈20-fold higher IL-8 secretion than the negative control. The secretion of IL-8 was significantly increased by both concentrations of *S. aureus* EVs and both concentrations of *S. epidermidis* EVs compared to the negative control or LTA. A dose-dependent increase in IL-8 secretion was detected for *S. epidermidis*-derived EVs. No significant differences were detected between groups treated with identical concentrations of *S. epidermidis*- and *S. aureus*-derived EVs.

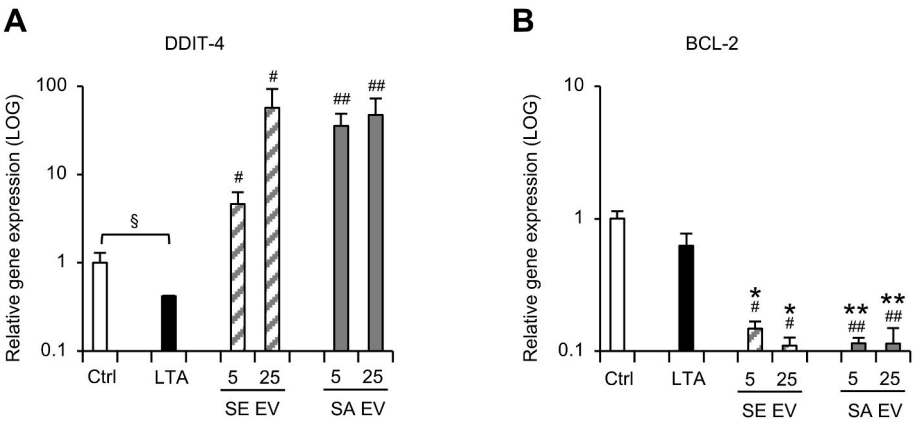

Fig. 4. The gene expression of THP-1 cells after a 24-h incubation with medium only (control; Ctrl), 5 μg × mL^{-1} lipoteichoic acid (LTA), or 5 μg × mL^{-1} or 25 μg × mL^{-1} *S. epidermidis* (SE)- or *S. aureus* (SA)-derived EVs determined by qPCR. A) DDIT4 and B) Bcl-2. Error bars show the standard error of the mean; $n = 3$ biological replicates. The bars for SE and SA represent the mean of 3 separate trials of each of the three (SE) and four (SA) clinical strains, respectively. Significant differences compared to control are indicated by asterisks: *$p < 0.05$; **<0.01. Significant differences compared to LTA are indicated by hash signs: $^{\#}p < 0.05$; $^{\#\#}p < 0.01$. Significant differences between different EV concentrations or EVs of different origins for an equivalent concentration are indicated by section sign: §<0.05.

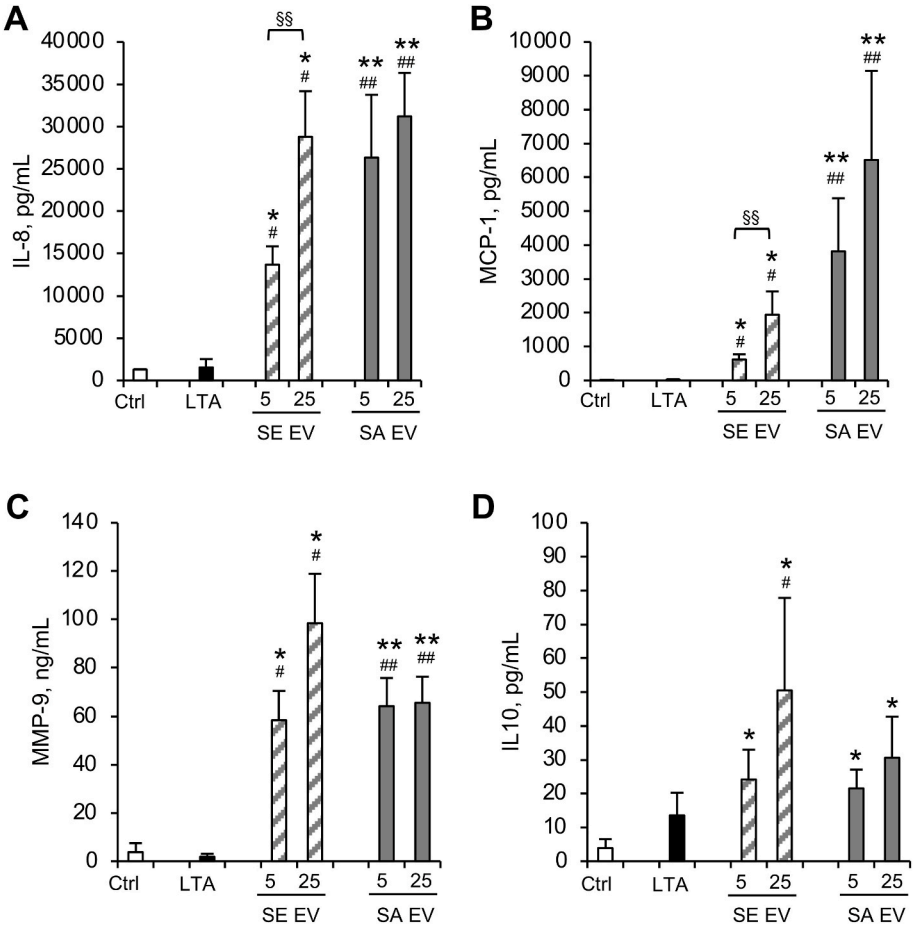

Fig. 5. The release of cytokines by THP-1 cells upon stimulation with 5 μg × mL^{-1} or 25 μg × mL^{-1} *S. epidermidis* (SE)- or *S. aureus* (SA)-derived EVs, 5 μg × mL^{-1} lipoteichoic acid (LTA) or medium only. (control; Ctrl) for 24 h was determined by ELISA. A) IL-8, B) MCP-1, C) MMP-9 and D) IL-10. Error bars show the standard error of the mean; $n = 3$ biological replicates. The bars for SE and SA represent the mean of 3 separate trials of each of the three (SE) and four (SA) clinical strains, respectively. Significant differences compared to control are indicated by asterisks: *$p < 0.05$; **<0.01. Significant differences compared to LTA are indicated by hash sign: $^{\#}p < 0.05$; $^{\#\#}p <$ 0.01. Significant differences between different EV concentrations or EVs of different origins for an equivalent concentration are indicated by section sign: §§<0.01.

For MCP-1, cytokine release was 6-fold and 3.3-fold higher for *S. aureus*-derived EVs than for *S. epidermidis*-derived EVs at the two different concentrations (Fig. 5B). The differences compared to the negative control group were 50- and 150-fold higher release for the *S. epidermidis* EV-treated groups (for 5 μg × mL^{-1} and 25 μg × mL^{-1}, respectively) and 300- and 500-fold higher release for the *S. aureus*-derived EV-treated groups (for 5 μg × mL^{-1} and 25 μg × mL^{-1}, respectively). All EV-treated groups (both *S. aureus*-derived and *S. epidermidis*-derived) were significantly different from both the negative and positive control groups. A dose-dependent increase in MCP-1 secretion was detected for *S. epidermidis*-derived EVs. No significant differences were detected between the groups treated with identical concentrations of *S. epidermidis*- and *S. aureus*-derived EVs.

Stimulation with EVs from *S. aureus* (5 and 25 μg × mL^{-1}) or *S. epidermidis* (5 and 25 μg × mL^{-1}) promoted a significant increase in MMP-9 secretion compared to stimulation with LTA or the negative control (Fig. 5C). The highest secretion of MMP-9 was achieved with *S. epidermidis* EVs at the highest concentration. No significant differences were detected between the groups treated with identical concentrations of *S. epidermidis*- and *S. aureus*-derived EVs.

All EV-stimulated groups demonstrated significantly higher IL-10 release than the negative control group. Only the highest concentration of *S. epidermidis* EVs promoted a significant increase in IL-10 compared with the positive control (Fig. 5D). No significant

differences were detected between the groups treated with identical concentrations of *S. epidermidis*- and *S. aureus*-derived EVs. Full data on the secretion of IL-8, MCP-1, MMP-9 and IL-10 by THP-1 cells induced by EVs from each individual clinical and reference strain are shown in Supplementary Figure S4.

3.8. NF-κB activation in cells

The activation of NF-κB was significantly higher for all EV-stimulated groups than for the negative control group at all time points (6, 12 and 24 h) (Fig. 6). A similar degree of NF-κB activation was observed for the EV-stimulated groups and the HKLM positive control group.

3.9. Internalization of EVs by THP-1 cells

To examine how *S. aureus*- and *S. epidermidis*-derived EVs interact with THP-1 cells, DiI-stained cells were incubated with DiO-stained *S. epidermidis*-derived EVs or DiO-stained *S. aureus*-derived EVs for 4 h and then observed under a confocal microscope. Both types of EVs were detected mainly in the cytoplasm of THP-1 cells, indicating internalization of both types of EVs into the cells at both concentrations and regardless of origin (Fig. 7A–D). No DiO staining was observed in the negative control group (Fig. 7E).

4. Discussion

During the last two decades, bacterial biofilms have been associated with persistent infection [18]. The precise pathogenic mechanism of infection related to orthopedic prostheses is, however, unknown. The main causative pathogens are staphylococci, and furthermore, multiple virulence factors have been implicated [19–21]. The present results demonstrated that *S. aureus* and *S. epidermidis,* which were isolated from implants and osteomyelitis near the implant site, had the ability to release EVs. These EVs exerted strong effects *in vitro* when delivered to THP-1 cells. The EVs activated NF-κB, promoted the gene expression and secretion of cytokines, were internalized, upregulated TLRs and induced cytolysis.

The current mechanism of the release of EVs from gram-positive bacteria is hypothesized to involve the action of cell wall-degrading enzymes that weaken the peptidoglycan layer, thereby facilitating EV release [22–24]. In the present study, the size of isolated EVs was larger than that reported previously for other *S. aureus*-derived EVs [15,16,25,26]. One explanation for the variability in EV size may be that although vesiculation is common among many bacterial species, EVs can be synthesized and regulated in different ways [22]. Other explanations include different isolation methods, different ultracentrifugation speeds and different filtration steps. EV size also varied among the strains evaluated. SEM analysis indicated a smaller vesicle size (≈30–100 nm for *S. epidermidis*-derived EVs) than that detected by NTA (≈30–180 nm). A possible explanation for the difference between the two methods is the preparation needed for SEM, which includes a dehydration step. Another explanation is that the NTA technique monitors EVs immersed in a fluid and equates the hydrodynamic diameter of analyzed particles, i.e., the EVs [27]. In addition, larger particles scatter light more strongly than smaller particles [28,29].

S. aureus displays multiple virulence factors, including different groups of toxins that are implicated in several diseases, such as α-hemolysin (α-toxin), γ-hemolysin, leukotoxins and phenol-soluble modulins (PSMs) [19,30]. *S. aureus*-induced cell death and caspase activation are mediated by α-toxin [31]. The present results demonstrated a dose-dependent reduction in THP-1 cell viability and prominent cell lysis (LDH release) after incubation with *S. aureus*-derived EVs. Previous proteomic studies have demonstrated that *S. aureus* EVs contain cargos with extracellular and membrane-associated virulence factors, including α-hemolysin and the γ-hemolysin component C toxins [11,32]. The current Western Blot results confirmed these findings as EVs from clinical and reference strains of *S. aureus* showed positive bands for several cytotoxins, such as α-hemolysin and δ-hemolysin, the protease Staphopain A, and Protein A. OMVs derived from gram-negative bacteria have been studied to a greater extent and for a longer time than EVs from gram-positive bacteria and are currently believed to deliver toxic cargos and virulence factors to target host cells [12,14,22,33].

In comparison with *S. aureus*-derived EVs, *S. epidermidis* EVs induced a less profound cytolytic effect on THP-1 cells. *S. epidermidis* is considered an opportunistic, low-pathogenicity bacterium, with biofilm formation as its main virulence mechanism [34]. Compared to that of

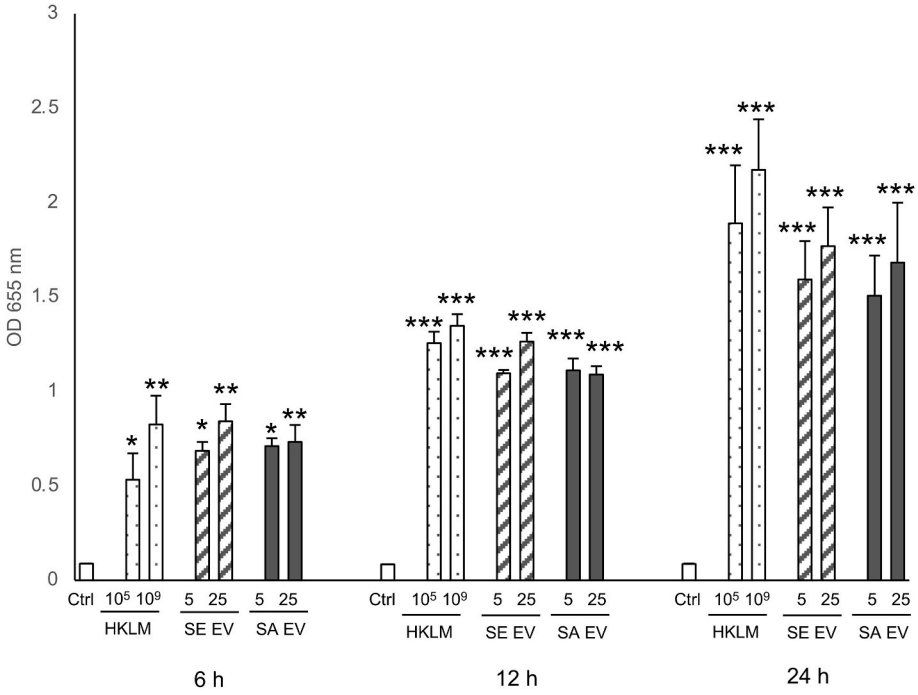

Fig. 6. SEAP levels detected due to NF-κB activation in THP1-Blue™ NF-κB cells at three time points, 6, 12 and 24 h, upon stimulation with 5 μg × mL^{-1} or 25 μg × mL^{-1} *S. epidermidis* (SE)- or *S. aureus* (SA)-derived EVs. Heat-killed *Listeria monocytogenes* (HKLM) and endotoxin-free water (Ctrl) served as the positive and negative controls, respectively. Error bars show the standard error of the mean; $n = 3$ biological replicates. The bars for SE and SA represent the mean of 3 separate trials of the clinical *S. epidermidis* CCUG 64521 and *S. aureus* CCUG 64516 strains, respectively. Significant differences compared to control are indicated by asterisks: asterisks: *$p < 0.05$; **$p < 0.01$; ***$p < 0.0001$.

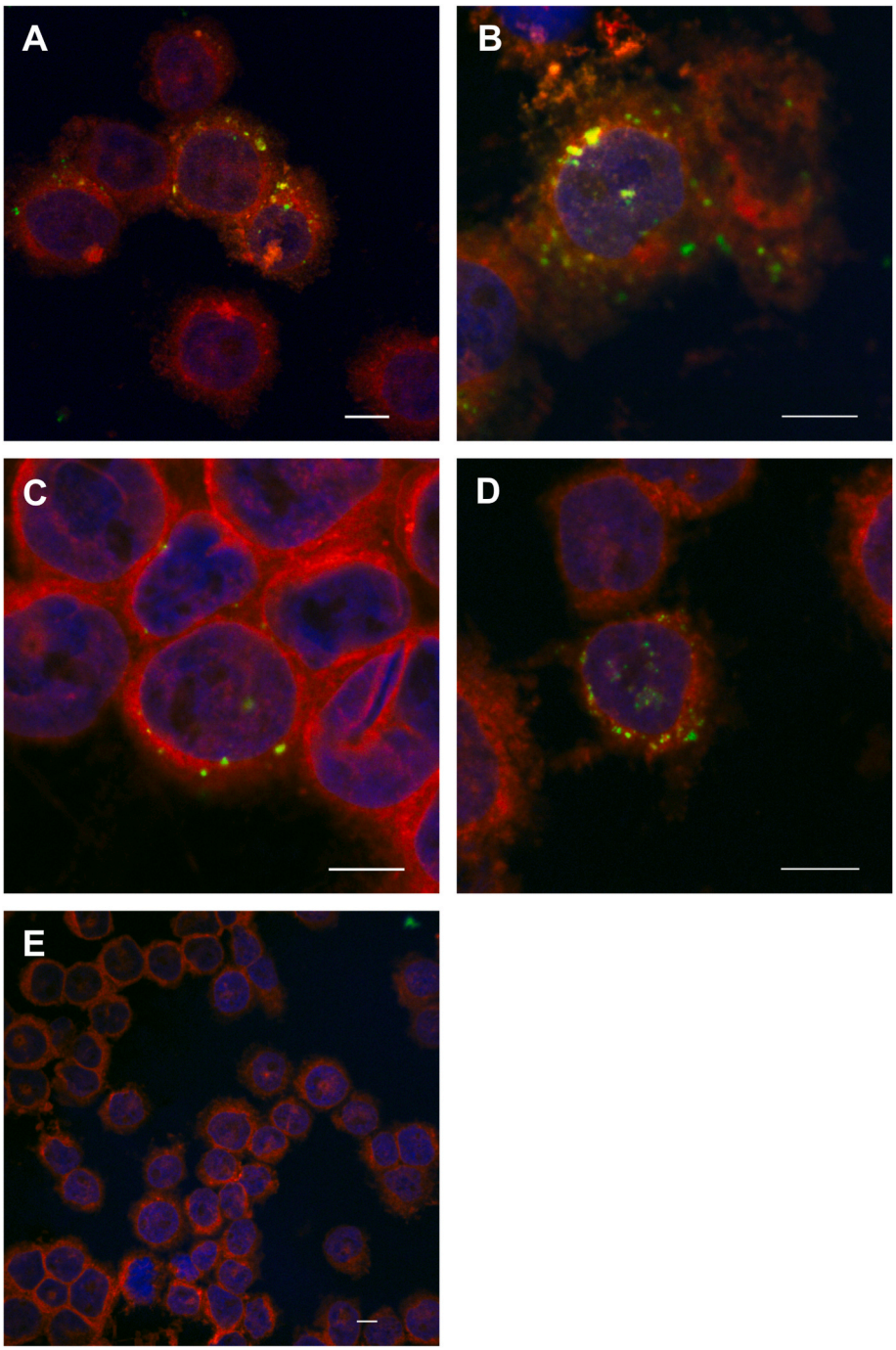

Fig. 7. CLSM showed that EVs derived from *S. aureus* (CCUG64520) (A–B) and *S. epidermidis* (CCUG64523) (C–D) clinical strains were internalized by THP-1 cells and localized mainly in the cytoplasm after 4 h. Green, DiO-stained EVs; red, DiI-stained THP-1 cell cytoplasm; blue, DAPI-stained nucleus of THP-1 cells. (A) and (C): 5 μg × mL^{-1} EVs; (B) and (D): 25 μg × mL^{-1} EVs. PBS served as the negative control (E). Scale bar: 10 μm.

S. aureus, *S. epidermidis* production of toxins is limited to PSMs, having noncytolytic and cytolytic (δ-toxin) properties [34,35]. In this study, we confirmed the presence of δ-toxin inside *S. epidermidis* EVs. PSM peptides in *S. epidermidis* form α-helices and fulfill requirements compatible with host cell membrane perturbation and pore formation, leading to cytolysis [35]. The composition of *S. epidermidis* EVs with respect to the presence of other PSMs and factors with a cytolytic capacity awaits proteomic studies since no information has been published to date.

In addition to the cytolytic effects of EVs, we explored the potential involvement of a few selected apoptosis-related factors, albeit at only the gene level. In the present study, increased DDIT4 gene expression was found after stimulation of THP-1 cells with EVs derived from either *S. aureus* or *S. epidermidis*. Together with the attenuated expression of Bcl-2, the results indicate that EVs have proapoptotic potential. DDIT4, also known as REDD1 or RTP801, encodes a protein with a molecular weight of 35 kDa [36,37]. It is induced by hypoxia, stress or DNA damage and exerts its function by inhibiting mammalian target of rapamycin (mTOR), a modulator of several biological functions, including cell growth, metabolism and immune responses [36–41]. DDIT4 is a proapoptotic mediator that inhibits mTOR [42], but its effects may vary depending on whether the cell is proliferating or fully differentiated [36,43] and whether the cell is subjected to hypoxic

preconditioning [44,45]. DDIT4 is one of the most commonly upregulated genes in transcriptomic studies on the effects of glucocorticoids on the brain or cells from the central nervous system [46] and is implicated in neurodegenerative diseases [42]. Furthermore, DDIT4 deficiency is possibly involved in the development of preeclampsia [47]. On the other hand, Bcl-2 is an antiapoptotic molecule that functions by binding to and suppressing nucleotide-dependent activator of cytokine-processing protease caspase-1 (NALP1), as well as suppressing caspase-1 activation and attenuating IL-1β production [48]. Previous findings have suggested the involvement of Bcl-2-regulated mechanisms in bacteria-induced cell apoptosis [31], whereas to the best of our knowledge, the enhanced DDIT4 expression induced by EVs represents the first observation of a link between bacteria/bacterial products and DDIT4, tentatively associated with host cell death. Future work will be aimed to determine the involvement of EV-induced cell apoptosis in addition to the direct cytolytic effects of EVs. Furthermore, it is of interest to determine whether EVs promote the upregulation of DDIT4 and inhibition of mTOR via interactions with TLRs to provide mechanistic insight into EV-induced cell death and cytokine release.

The migration of leukocytes, initially polymorphonuclear leukocytes (PMNs) and later monocytes, from the microvasculature into the site of infection is largely believed to be directed by chemokinetic and chemotactic factors secreted from cells during encounters with bacterial products. Here, EVs derived from both *S. aureus* and *S. epidermidis* were shown to be potent inducers of the cascade of important proinflammatory and immunomodulatory chemokines and cytokines, which was demonstrated at the gene and protein levels. Moreover, for the first time, EVs derived from *S. epidermidis* were found to induce dose-dependent expression and secretion of IL-8, a chemoattractant for PMNs, and MCP-1, a chemoattractant for monocytes/macrophages. Likewise, *S. epidermidis* bacteria promote the recruitment of inflammatory cells (mainly PMNs), cell death and gene expression of TNF-α, IL-6, IL-8, TLR2 and elastase in association with implants *in vivo* [49].

Interestingly, no statistically significant differences in the ability to induce the secretion of IL-8, MCP-1, MMP-9 or IL-10 were detected between equivalent concentrations of EVs from *S. aureus* and *S. epidermidis*. In addition, there were no statistically significant differences between EVs from infected orthopedic amputation prostheses and those from reference strains in regard to the ability to induce secretion of these chemokines and cytokines by THP-1 cells. This may seem at variance with the scientific and clinical notions that *S. aureus* infection typically has an acute and aggressive course by virtue of multiple virulence factors, whereas *S. epidermidis* presents with a less aggressive and more chronic nature, with its pathogenicity mainly related to biofilm formation [4,50]. It is evident, however, that additional information on the kinetics of cytokine production and secretion is needed for EVs from each source. With respect to the mechanism of EV-induced cytokine secretion, there is a scarcity of information in the previously published literature on *S. aureus* EVs. On the other hand, previous studies have demonstrated that treatment of human PMNs with LTA from *S. aureus* induces secretion of IL-8 by PMNs via CD14 and TLR2 and NF-κB activation [51]. Here, our results provide an indication that the cytokine and chemokine expression and secretion induced by EVs involve the activation of the transcription factor NF-κB. Interestingly, the major upregulation of TLRs was mainly related to TLR3. To decipher the roles of TLRs as well as the role of internalization implicated in EV activation of THP-1 cells, further studies are required. Moreover, the effects of staphylococcal EVs on inflammatory cell chemotaxis, cytokine secretion, and phagocytosis and the fates of EVs and staphylococci in biomaterial-associated infection *in vivo* need to be determined.

Both types of EVs induced MMP-9 gene expression and secretion by THP-1 cells. MMP-9 is expressed and activated in response to tissue damage and TNF-α [52,53]. Both MMP-9 and elastase have been implicated in the degradation of the basement membrane, thus facilitating PMN transmigration across the blood vessel wall [54]. Whether *S. aureus* and *S. epidermidis* EVs contribute not only to inflammation but also to extracellular matrix degradation and tissue remodeling via EV-induced MMP-9 secretion awaits further investigation.

EVs derived from either *S. aureus* or *S. epidermidis* were internalized by monocytic THP-1 cells. This finding corroborates observations made in other studies, showing internalization of gram-positive EVs by different eukaryotic cell types [16,55,56]. However, the vesicles were not internalized by all cells. To understand the importance of the internalization process for the induction of cytolysis and cytokine secretion, additional experiments, for example, blocking cell-surface receptors and inhibiting internalization processes, are of interest.

A major limitation of the present study was the relatively small size of the patient cohort. Nevertheless, we obtained hitherto available samples from patients with bone-anchored amputation prostheses who were diagnosed with osteomyelitis [57,58]. Among the samples, both *S. aureus* and *S. epidermidis* demonstrated biofilm formation *in vitro* but to varying degrees. Since biofilm formation is considered an important mechanism to evade host defense, the relations between the *S. epidermidis* or *S. aureus* biofilm formation ability and the amount of released EVs and their cytolytic and cytokine secretion-inducing effects could not be determined. An ongoing study using a larger patient cohort with infections associated with total hip replacement will allow such determination [59].

The present study utilized a monocytic cell line to evaluate the cytotoxicity, internalization and cytokine secretion induced by EVs. Although this is a commonly used cell type, the effects of EVs on primary cells, including human PMNs, monocytes and macrophages, remain to be established.

Strategies to minimize the occurrence of biomaterial-associated infection require a deeper understanding of both material-related factors and biological processes. *S. aureus* and coagulase-negative staphylococci account for the majority of orthopedic implant infections and possess an impressive armamentarium for adhesion, colonization, invasion, persistence, antimicrobial resistance and evasion of host defense. In the present *in vitro* study, all seven investigated *S. aureus* and *S. epidermidis* strains obtained from deep infections of osseointegrated amputation prostheses were able to release EVs irrespective of whether they were characterized as strong, moderate or weak producers or nonproducers of biofilms. Depending on the parental cell, the cytolytic effect on THP-1 cells was more strongly induced by *S. aureus* EVs. In contrast, both types of EVs were internalized and elicited pronounced secretion of IL-8, MCP-1, MMP-9 and IL-10, all known to be secreted at titanium implant surfaces *in vivo* after challenge with staphylococci [49].

5. Conclusions

The present study provides evidence that staphylococci isolated from infected bone-anchored prostheses secrete EVs under planktonic conditions *in vitro*. By virtue of the potent immunomodulatory and toxic effects exerted on monocytes, further studies on the role of EVs in the pathogenesis of implant-related infection and loosening of prostheses are urgently required.

Author contributions

MZ, MT, PT: Conceptualization; MZ, FV, FAS, RF, OO, KE, MT: Data curation; MZ, FV, FAS, RF, OO, KE, MT, PT: Formal analysis; PT, OO, MT: Funding acquisition; MZ, MT, RF, KE, PT: Investigation; MZ, FV, RF, KE, MT: Methodology; MZ, MT, KE, PT: Project administration; KE, MT, PT: Supervision; MZ, FAS, RF, OO: Visualization; MZ: Writing - original draft; FV, FAS, RF, OO, KE, MT, PT: Writing - review & editing.

Declaration of competing interest

The authors declare that they have no known competing financial interests or personal relationships that could have appeared to influence

the work reported in this paper.

Acknowledgments

The authors would like to express their appreciation to Anna Johansson and Maria Hoffman for their expert technical assistance. The support from the Swedish Research Council (2018-02891), the Swedish state under the agreement between the Swedish government and the county councils, the ALF agreement (ALFGBG-725641; “Optimization of osseointegration for treatment of transfemoral amputees”), the European Union’s Horizon 2020 research and innovation program under the Marie Skłodowska-Curie grant agreement No. 754412 (MoRE2020 - Region Västra Götaland), CARe - Centre for Antibiotic Resistance Research at University of Gothenburg, the IngaBritt and Arne Lundberg Foundation, the Eivind and Elsa K: son Sylvan Foundation, the Hjalmar Svensson Foundation, the Adlerbertska Foundation, the Doctor Felix Neubergh Foundation, and the Area of Advance Materials of Chalmers and GU Biomaterials within the Strategic Research Area initiative launched by the Swedish government is gratefully acknowledged. FAS was supported by a postdoctoral scholarship from Svenska Sällskapet för Medicinsk Forskning (SSMF), a Young Researcher Grant from the Osteology Foundation, Switzerland, and a grant from Konrad and Helfrid Johansson’s Foundation. The authors confirm that there are no known conflicts of interest associated with the publication and that there was no significant financial support for this work that could have influenced its outcome. The sponsors were not involved in the study design; data acquisition; or interpretation, writing or submission of the article.

Appendix A. Supplementary data

Supplementary data to this article can be found online at https://doi.org/10.1016/j.biomaterials.2021.121158.

References

[1] A. Palmquist, O.M. Omar, M. Esposito, J. Lausmaa, P. Thomsen, Titanium oral implants: surface characteristics, interface biology and clinical outcome, J. R. Soc. Interface 7 (Suppl 5) (2010) S515–S527.
[2] J.M. Anderson, A. Rodriguez, D.T. Chang, Foreign body reaction to biomaterials, Semin. Immunol. 20 (2) (2008) 86–100.
[3] H.J. Busscher, H.C. van der Mei, G. Subbiahdoss, P.C. Jutte, J.J. van den Dungen, S. A. Zaat, M.J. Schultz, D.W. Grainger, Biomaterial-associated infection: locating the finish line in the race for the surface, Sci. Transl. Med. 4 (153) (2012) 153rv10.
[4] C. Arciola, D. Campoccia, L. Montanaro, Implant Infections: Adhesion, Biofilm Formation and Immune Evasion, Nature Publishing Group, London, 2018, pp. 397–409.
[5] R.O. Darouiche, Device-Associated Infections: a macroproblem that starts with microadherence, Clin. Infect. Dis. 33 (2001) 1567–1572.
[6] R.O. Darouiche, Treatment of infections assoiciated with surgical implants, N. Engl. J. Med. 350 (14) (2004) 1422–1429.
[7] G. Stocks, H.F. Janssen, Infection in patients after implantation of an orthopedic device, ASAIO J 46 (6) (2000) S41–S46.
[8] M. Sj, R.P. Howlin, G. Jf, M. Mm, C. Jh, Biofilms in periprosthetic orthopedic infections, Future Microbiol. 9 (2014) 987–1007.
[9] W. Zimmerli, C. Moser, Pathogenesis and treatment concepts of orthopaedic biofilm infections, FEMS Immunol. Med. Microbiol. 65 (2) (2012) 158–168.
[10] G.A. Duque, A. Descoteaux, Macrophage cytokines: involvement in immunity and infectious diseases, Front. Immunol. 5 (2014) 1–12.
[11] E.Y. Lee, D.Y. Choi, D.K. Kim, J.W. Kim, J.O. Park, S. Kim, S.H. Kim, D. M. Desiderio, Y.K. Kim, K.P. Kim, Y.S. Gho, Gram-positive bacteria produce membrane vesicles: proteomics-based characterization of Staphylococcus aureus-derived membrane vesicles, Proteomics 9 (24) (2009) 5425–5436.
[12] J. Km, C. Kn, Bacterial outer membrane vesicles and the host-pathogen interaction, Genes Dev. 19 (22) (2005) 2645–2655.
[13] J.M. Bomberger, D.P. MacEachran, B.A. Coutermarsh, S. Ye, G.A. O’Toole, B. A. Stanton, Long-distance delivery of bacterial virulence factors by Pseudomonas aeruginosa outer membrane vesicles, PLoS Pathog. 5 (4) (2009).
[14] T.N. Ellis, M.J. Kuehn, Virulence and immunomodulatory roles of bacterial outer membrane vesicles, Microbiol. Mol. Biol. Rev. 74 (1) (2010) 81–+.
[15] M. Gurung, D.C. Moon, C.W. Choi, J.H. Lee, Y.C. Bae, J. Kim, Y. Lee, S. Seol, D. Cho, S. Kim, J. Lee, Staphylococcus aureus produces membrane-derived vesicles that induce host cell death, PloS One 6 (11) (2011).
[16] S.W. Hong, M.R. Kim, E.Y. Lee, J.H. Kim, Y.S. Kim, S.G. Jeon, J.M. Yang, B.J. Lee, B.Y. Pyun, Y.S. Gho, Y.K. Kim, Extracellular vesicles derived from Staphylococcus aureus induce atopic dermatitis-like skin inflammation, Allergy 66 (3) (2011) 351–359.
[17] J. Lee, E.Y. Lee, S.H. Kim, D.K. Kim, K.S. Park, K.P. Kim, Y.K. Kim, T.Y. Roh, Y. S. Gho, Staphylococcus aureus extracellular vesicles carry biologically active beta-lactamase, Antimicrob. Agents Chemother. 57 (6) (2013) 2589–2595.
[18] J.W. Costerton, P.S. Stewart, E.P. Greenberg, Bacterial biofilms: a common cause of persistent infections, Science 284 (5418) (1999) 1318–1322.
[19] D. Oliveira, A. Borges, M. Simoes, Staphylococcus aureus toxins and their molecular activity in infectious diseases, Toxins 10 (6) (2018).
[20] M. Otto, Molecular basis of Staphylococcus epidermidis infections, Semin. Immunopathol. 34 (2) (2012) 201–214.
[21] M. Otto, Staphylococcal infections: mechanisms of biofilm maturation and detachment as critical determinants of pathogenicity, Annu. Rev. Med. 64 (2013) 175–188.
[22] L. Brown, J.M. Wolf, R. Prados-Rosales, A. Casadevall, Through the wall: extracellular vesicles in Gram-positive bacteria, mycobacteria and fungi, Nat. Rev. Microbiol. 13 (10) (2015) 620–630.
[23] J.H. Kim, J. Lee, J. Park, Y.S. Gho, Gram-negative and Gram-positive bacterial extracellular vesicles. Seminars in Cell & Developmental Biology, 2015.
[24] Y. Liu, K.A.Y. Defourny, E.J. Smid, T. Abee, Gram-positive bacterial extracellular vesicles and their impact on health and disease, Front. Microbiol. 9 (1502) (2018) 1–8.
[25] B. Thay, S. Wai, J. Oscarsson, Staphylococcus aureus a-toxin-dependent induction of host cell death by membrane-derived vesicles, PloS One 8 (1) (2013).
[26] E.-Y. Lee, D.-Y.- Choi, D.-K. Kim, J.-W. Kim, J.O. Park, S.H. Kim, S.-H. Kim, D. M. Desiderio, Y.-K. Kim, K.-P. Kim, Y.S. Gho, Gram-positive bacteria produce membrane vesicles: proteomics-based characterization of Staphylococcus aureus-derived membrane vesicles, Proteomics 9 (24) (2009) 5425–5436.
[27] T. Jani, J.H.J. Ann-Cathrin, H. Jenny Perez, G. Stefan, A.G.-U. Julián, O. Eva, B.C. P. Jan, H. Martin, Intermethod comparison of the particle size distributions of colloidal silica nanoparticles, Sci. Technol. Adv. Mater. 15 (3) (2014), 035009.
[28] V.S. Chernyshev, R. Rachamadugu, Y.H. Tseng, D.M. Belnap, Y.L. Jia, K.J. Branch, A.E. Butterfield, L.F. Pease, P.S. Bernard, M. Skliar, Size and shape characterization of hydrated and desiccated exosomes, Anal. Bioanal. Chem. 407 (12) (2015) 3285–3301.
[29] V. Sokolova, A.K. Ludwig, S. Hornung, O. Rotan, P.A. Horn, M. Epple, B. Glebel, Characterisation of exosomes derived from human cells by nanoparticle tracking analysis and scanning electron microscopy, Colloids Surf. B Biointerfaces 87 (1) (2011) 146–150.
[30] D. Grumann, U. Nubel, B.M. Broker, Staphylococcus aureus toxins - their functions and genetics, Infect. Genet. Evol. 21 (2014) 583–592.
[31] H. Bantel, B. Sinha, W. Domschke, G. Peters, K. Schulze-Osthoff, R.U. Janicke, alpha-Toxin is a mediator of Staphylococcus aureus-induced cell death and activates caspases via the intrinsic death pathway independently of death receptor signaling, The Journal of cell biology 155 (4) (2001) 637–648.
[32] H. Jeon, M.H. Oh, S.H. Jun, S. Il Kim, C.W. Choi, H.I. Kwon, S.H. Na, Y.J. Kim, A. Nicholas, G.N. Selasi, J.C. Lee, Variation among Staphylococcus aureus membrane vesicle proteomes affects cytotoxicity of host cells, Microb. Pathog. 93 (2016) 185–193.
[33] M. Gurung, D.C. Moon, C.W. Choi, J.H. Lee, Y.C. Bae, J. Kim, Y.C. Lee, S.Y. Seol, D. T. Cho, S.I. Kim, J.C. Lee, Staphylococcus aureus produces membrane-derived vesicles that induce host cell death, PloS One 6 (11) (2011).
[34] M. Otto, Staphylococcus epidermidis–the ’accidental’ pathogen, Nat. Rev. Microbiol. 7 (8) (2009) 555–567.
[35] G.Y. Cheung, K. Rigby, R. Wang, S.Y. Queck, K.R. Braughton, A.R. Whitney, M. Teintze, F.R. DeLeo, M. Otto, Staphylococcus epidermidis strategies to avoid killing by human neutrophils, PLoS Pathog. 6 (10) (2010), e1001133.
[36] T. Shoshani, A. Faerman, I. Mett, E. Zelin, T. Tenne, S. Gorodin, Y. Moshel, S. Elbaz, A. Budanov, A. Chajut, H. Kalinski, I. Kamer, A. Rozen, O. Mor, E. Keshet, D. Leshkowitz, P. Einat, R. Skaliter, E. Feinstein, Identification of a novel hypoxia-inducible factor 1-responsive gene, RTP801, involved in apoptosis, Mol. Cell Biol. 22 (7) (2002) 2283.
[37] L.W. Ellisen, K.D. Ramsayer, C.M. Johannessen, A. Yang, H. Beppu, K. Minda, J. D. Oliner, F. McKeon, D.A. Haber, REDD1, a developmentally regulated transcriptional target of p63 and p53, links p63 to regulation of reactive oxygen species, Mol. Cell. 10 (5) (2002) 995–1005.
[38] F. Schmitz, A. Heit, S. Dreher, K. Eisenächer, J. Mages, T. Haas, A. Krug, K. P. Janssen, C.J. Kirschning, H. Wagner, Mammalian target of rapamycin (mTOR) orchestrates the defense program of innate immune cells, Eur. J. Immunol. 38 (11) (2008) 2981–2992.
[39] J.D. Powell, K.N. Pollizzi, E.B. Heikamp, M.R. Horton, Regulation of immune responses by mTOR, Annu. Rev. Immunol. 30 (1) (2012) 39–68.
[40] J.D. Powell, G.M. Delgoffe, The mammalian target of rapamycin: linking T cell differentiation, function, and metabolism, Immunity 33 (3) (2010) 301–311.
[41] T. Weichhart, M. Hengstschlager, M. Linke, Regulation of innate immune cell function by mTOR.(mammalian target of rapamycin)(Report), Nat. Rev. Immunol. 15 (10) (2015) 599.
[42] M. Canal, J. Romaní-Aumedes, N. Martín-Flores, V. Pérez-Fernández, C. Malagelada, RTP801/REDD1: a stress coping regulator that turns into a troublemaker in neurodegenerative disorders, Front. Cell. Neurosci. 8 (2014) 313.
[43] C. Malagelada, E.J. Ryu, S.C. Biswas, V. Jackson-Lewis, L.A. Greene, RTP801 is elevated in Parkinson brain substantia nigral neurons and mediates death in cellular models of Parkinson’s disease by a mechanism involving mammalian target of rapamycin inactivation, J. Neurosci. : the official journal of the Society for Neuroscience 26 (39) (2006) 9996.

[44] M. Gustavsson, M.A. Wilson, C. Mallard, C. Rousset, M.V. Johnston, H. Hagberg, Global gene expression in the developing rat brain after hypoxic preconditioning: involvement of apoptotic mechanisms? Pediatr. Res. 61 (4) (2007), 444-.50 61(4) (2007) 444-50.
[45] S. Rolf, T. Daniel, A. Wolfgang, G. Klaus, K. Anke, K. Jörg, REDD1 integrates hypoxia-mediated survival signaling downstream of phosphatidylinositol 3-kinase, Oncogene 24 (7) (2004) 1138.
[46] G.R. Juszczak, A.M. Stankiewicz, Glucocorticoids, genes and brain function, Progress in Neuropsychopharmacology & Biological Psychiatry 82 (2018) 136–168.
[47] J. Yang, Y. Zhang, J. Tong, H. Lv, C. Zhang, Z.-J. Chen, Dysfunction of DNA damage-inducible transcript 4 in the decidua is relevant to the pathogenesis of preeclampsia, Biol. Reprod. 98 (6) (2018) 821.
[48] J.-M. Bruey, N. Bruey-Sedano, F. Luciano, D. Zhai, R. Balpai, C. Xu, C.L. Kress, B. Bailly-Maitre, X. Li, A. Osterman, S.-I. Matsuzawa, A.V. Terskikh, B. Faustin, J. C. Reed, Bcl-2 and Bcl-XL regulate proinflammatory caspase-1 activation by interaction with NALP1, Cell 129 (1) (2007) 45.
[49] S. Svensson, M. Trobos, M. Hoffman, B. Norlindh, S. Petronis, J. Lausmaa, F. Suska, P. Thomsen, A novel soft tissue model for biomaterial-associated infection and inflammation – Bacteriological, morphological and molecular observations, Biomaterials 41 (2015) 106–121.
[50] T.J. Foster, Immune evasion by staphylococci, Nat. Rev. Microbiol. 3 (12) (2005) 948–958.
[51] S. Lotz, E. Aga, I. Wilde, G. van Zandbergen, T. Hartung, W. Solbach, T. Laskay, Highly purified lipoteichoic acid activates neutrophil granulocytes and delays their spontaneous apoptosis via CD14 and TLR2, J. Leukoc. Biol. 75 (3) (2004) 467–477.
[52] Y.P. Han, T.L. Tuan, M. Hughes, H. Wu, W.L. Garner, Transforming growth factor-beta - and tumor necrosis factor-alpha -mediated induction and proteolytic activation of MMP-9 in human skin, J. Biol. Chem. 276 (25) (2001) 22341–22350.
[53] A. Voss, K. Gescher, A. Hensel, W. Nacken, C. Kerkhoff, Double-stranded RNA induces MMP-9 gene expression in HaCaT keratinocytes by tumor necrosis factor-alpha, Inflamm. Allergy - Drug Targets 10 (3) (2011) 171–179.
[54] C. Delclaux, C. Delacourt, M.P. D'Ortho, V. Boyer, C. Lafuma, A. Harf, Role of gelatinase B and elastase in human polymorphonuclear neutrophil migration across basement membrane, Am. J. Respir. Cell Mol. Biol. 14 (3) (1996) 288–295.
[55] M.R. Kim, S.W. Hong, E.B. Choi, W.H. Lee, Y.S. Kim, S.G. Jeon, M.H. Jang, Y. S. Gho, Y.K. Kim, Staphylococcus aureus-derived extracellular vesicles induce neutrophilic pulmonary inflammation via both Th1 and Th17 cell responses, Allergy 67 (10) (2012) 1271–1281.
[56] M.V. Surve, A. Anil, K.G. Kamath, S. Bhutda, L.K. Sthanam, A. Pradhan, R. Srivastava, B. Basu, S. Dutta, S. Sen, D. Modi, A. Banerjee, Membrane vesicles of group B Streptococcus disrupt feto-maternal barrier leading to preterm birth, PLoS Pathog. 12 (9) (2016).
[57] M. Lenneras, G. Tsikandylakis, M. Trobos, O. Omar, F. Vazirisani, A. Palmquist, O. Berlin, R. Branemark, P. Thomsen, The clinical, radiological, microbiological, and molecular profile of the skin-penentration site of transfemoral amputees treated with bone-anchored prostheses, J. Biomed. Mater. Res. 105A (2017) 578–589.
[58] M. Zaborowska, J. Tillander, R. Branemark, L. Hagberg, P. Thomsen, Biofilm formation and antimicrobial susceptibility of staphylococci and enterococci from osteomyelitis associated with percutaneous orthopaedic implants, J. Biomed. Mater. Res. Part B 105B (2017) 2630–2640.
[59] J. Kärrholm, The Swedish hip arthroplasty register, Acta Orthop. 81 (1) (2010) 3–4. www.shpr.se.